Chinese Journal of Aeronautics, 2013,26(2): 350–356

Chinese Society of Aeronautics and Astronautics
& Beihang University

Chinese Journal of Aeronautics

cja@buaa.edu.cn
www.sciencedirect.com

Independent modal variable structure fuzzy active vibration control of thin plates laminated with photostrictive actuators

He Rongbo [a,b], Zheng Shijie [a,*]

[a] *Institute of Smart Materials and Structures, State Key Laboratory of Mechanics and Control of Mechanical Structures, Nanjing University of Aeronautics and Astronautics, Nanjing 210016, China*
[b] *School of Electrical Information, Anhui University of Technology, Ma'anshan 243002, China*

Received 29 November 2011; revised 8 February 2012; accepted 14 March 2012
Available online 6 March 2013

KEYWORDS

Fuzzy active control;
Independent modal;
Photostrictive actuators;
Thin plate vibration;
Variable structure

Abstract Photostrictive actuators can produce photodeformation strains under illumination of ultraviolet lights. They can realize non-contact micro-actuation and vibration control for elastic plate structures. Considering the switching actuation and nonlinear dynamic characteristics of photostrictive actuators, a variable structure fuzzy active control scheme is presented to control the light intensity applied to the actuators. Firstly, independent modal vibration control equations of photoelectric laminated plates are established based on modal analysis techniques. Then, the optimal light switching function is derived to increase the range of sliding modal area, and the light intensity self-adjusting fuzzy active controller is designed. Meanwhile, a continuous function is applied to replace a sign function to reduce the variable structure control (VSC) chattering. Finally, numerical simulation is carried out, and simulation results indicate that the proposed control strategy provides better performance and control effect to plate actuation and control than velocity feedback control, and suppresses vibration effectively.

1. Introduction

With its unique mechanisms of energy conversion, a photostrictive actuator is immune from the electromagnetic interferences, and can realize non-contact micro-actuation and vibration control for elastic structures. In addition, it requires no additional high voltage or strong magnetic generating equipment. It can realize light-weight, small size applications, and is especially used for control signal transmission and active control in vacuum and outer space environment. Photostrictive actuators made up of lanthanum-modified lead zirconate titanate (PLZT) ceramics have received increased attentions with many advantages over conventional electro-mechanical actuators, such as non-contact actuation, remote control, and immunity from electric/magnetic disturbances. Tzou and Chou,[1] Shih and Tzou[2] investigated the constitutive model and the coupling behaviors of photostriction, photodeformation, pyroelectricity,

* Corresponding author. Tel.: +86 25 84893491 186.
E-mail addresses: hrb100200@163.com (R. He), sjzheng@nuaa.edu.cn (S. Zheng).

Peer review under responsibility of Editorial Committe of CJA.

ELSEVIER Production and hosting by Elsevier

1000-9361 © 2013 Production and hosting by Elsevier Ltd. on behalf of CSAA & BUAA. Open access under CC BY-NC-ND license.
http://dx.doi.org/10.1016/j.cja.2013.02.012

thermoelasticity, and opto-piezothermoelasticity for one- and two-dimensional distributed photostrictive actuators. Liu and Tzou[3] proposed a wireless vibration control method of plates using distributed photostrictive actuators. Since the pioneering work of Liu and Tzou, some researchers have investigated vibration control of beams, plates, and various kinds of shells using photostrictive actuators with uniform illumination.[4–9] Yue et al.[10] explored a new multiple degree-of-freedom (multi-DOF) distributed actuator configuration spatially bonded on the surface of shell structures to enhance the spatial modal controllability. Sun and Tong[11] presented analytical investigation on wireless remote vibration control of flexible beams with a non-linear exponential model of photostrictive film actuators. Very recently, Zheng[12] carried out finite element simulation of wireless structural vibration control with photostrictive actuators. Chen and Zheng[13] presented a novel binary-coded genetic algorithm (GA) based linear quadratic regulator (LQR) control scheme.

It is noteworthy that the characteristic of active vibration control using photostrictive actuators is different from that using usual piezoelectric actuators. The major difference is that the light intensity applied to photostrictive actuators is always positive and the deformation of photostrictive actuators is always tensile. So the light illumination should be alternatively applied to the top and bottom photostrictive actuators. In view of switching actuation, variable structure control (VSC) action takes place. Variable structure control is basically a control law that switches rapidly between two values or gains, with an objective of bringing the system's state trajectory onto a specified surface, called the sliding surface. To achieve variable structure control successfully, it is key to choose the switching surface. Furthermore, a major drawback of VSC in practical applications is the chattering problem. However, the optimal sliding surface and chattering problem for wireless vibration control have not been discussed. Moreover, as far as the authors are aware, most of past work in the area of wireless vibration control has focused on applications of two control algorithms[3,5,6,9] (i.e., variable light intensity control and constant light intensity control), and most of the novel emerging control methods have not been applied to wireless vibration control. Fuzzy logic control has emerged as one of the most active and fruitful approaches to deal with complex and ill-defined dynamic systems.[14,15] The motivation is often due to the fact that system knowledge and dynamic behavior are qualitative and uncertain, so the fuzzy set theory appears to provide a suitable representation of such knowledge. Usually, the qualitative knowledge is firstly represented by fuzzy sets, and then, by using a compositional rule of inference and approximate reasoning, a fuzzy control law can be constructed. Compared to conventional control theories, fuzzy logic control does not rely on the analysis of a mathematical model of a plant. In essence, fuzzy logic can emulate human thinking and organize the approximate and indeterminate natures of the environment. Though this method has not been viewed as a rigorous theory, it is believed that the basic idea behind the approach would have a significant influence on the practice of controlling complex systems vibration in the future.

This paper presents an investigation into the variable structure fuzzy active vibration control of a simply supported rectangular plate using photostrictive actuators. The paper is organized as follows. Section 2 introduces a mathematical model of a thin plate laminated with photostrictive actuators. The proposed variable structure fuzzy active control algorithm is presented in Section 3. Numerical simulation results are shown in Section 4, and Section 5 concludes this paper.

2. Modeling of thin plate laminated with photostrictive actuators

Two pairs of photostrictive actuators are respectively placed on the top and bottom surfaces of a simply supported isotropic plate, as shown in Fig. 1. The photostrictive actuators are assumed not to significantly alter the inertial mass and effective stiffness of the base plate structure.

The results of Ref.[6] reveal that effective control depends on the locations of actuators. In detail, in order to ensure the controllability for most of the vibration modes, the actuators need to be placed unsymmetrically at the $L_x/2$ and $L_y/2$ lines. In this paper, it is assumed that the polarity directions of the surface-bonded actuator patches 1 and 2 are in the x-direction and y-direction, respectively. Their placements are defined by edge coordinates, x_1^x, x_2^x, y_1^x, y_2^x and x_1^y, x_2^y, y_1^y, y_2^y. When the patches are activated, the induced bending moment M_{xx}^{a} and M_{yy}^{a} along the different polarity directions can be derived using the unit step function.[6]

Substituting the modal expression written as a summation of sinusoidal modes into the system equation leads to an equation in term of the modal coordinate. Integrating over the whole plate surface, applying the modal orthogonality of natural modes, the modal equation can be written as[6]

$$\ddot{\eta}_{mn} + 2\zeta_{mn}\omega_{mn}\dot{\eta}_{mn} + \omega_{mn}^2\eta_{mn} = F_{mn}^{\mathrm{c}} \tag{1}$$

where η_{mn} is the plate response amplitude of the mnth mode, ζ_{mn} the damping ratio, ω_{mn} the natural frequency of the mnth mode, and F_{mn}^{c} is the modal control force, which is defined as

$$F_{mn}^{\mathrm{c}} = -(\tilde{M}_{mnx} + \tilde{M}_{mny})\bar{S}(t) \tag{2}$$

where $\bar{S}(t)$ is the photodeformation strain of the photostrictive actuator, and

$$\begin{cases} \tilde{M}_{mn\dagger} = \dfrac{2(h+h_{\mathrm{a}})h_{\mathrm{a}}Y_{\mathrm{a}}}{\rho h L_x L_y}\langle\dagger\rangle[\![\,\dagger\,]\!] \quad \dagger = x, y \\ \langle x\rangle = \dfrac{mL_y}{nL_x} \\ \langle y\rangle = \dfrac{nL_x}{mL_y} \\ [\![\,\dagger\,]\!] = \left(\cos\dfrac{m\pi x_1}{L_x} - \cos\dfrac{m\pi x_2^{\dagger}}{L_x}\right)\left(\cos\dfrac{n\pi y_1^{\dagger}}{L_y} - \cos\dfrac{n\pi y_2^{\dagger}}{L_y}\right) \end{cases} \tag{3}$$

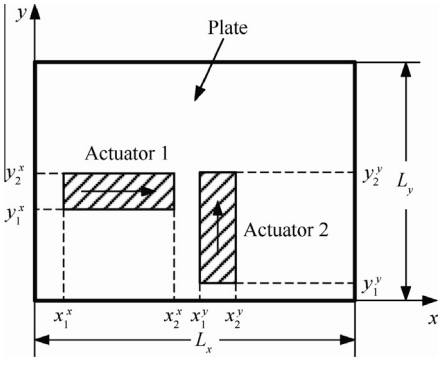

Fig. 1 Plate with surface-bonded actuators.

where Y_a is the elastic modulus of the actuator, h_a the actuator thickness, h the plate thickness, ρ the density of plate.

The photodeformation effect induced by the photostrictive actuator is defined by[6]

$$\bar{S}(t) = d_{33}E(t) - \lambda\theta(t)/Y_a \tag{4}$$

where d_{33} is the piezoelectric-strain constant, λ a thermal stress coefficient, $E(t)$ the total induced electric field including both the photovoltaic effect and the pyroelectric effect, $\theta(t)$ the temperature change of the photostrictive actuator due to the high-energy illumination. The detailed expression of $E(t)$ and $\theta(t)$ can be referred to Ref. 6.

3. Independent modal variable structure fuzzy active control design

3.1. Light switching function design

As mentioned previously, the paired photostrictive actuators are respectively placed on the top and bottom surfaces of the plate. By activating the light sources alternatively, both positive and negative control actions can be generated. It is apparent that the alternate mode of light illumination is important. In this paper, light switching function is taken as the following linear function:

$$s = c\eta + \dot{\eta} \tag{5}$$

where c is a positive constant, which is simply the slope of the switching surface. When the light illumination is alternatively varied with the sign of the switching function, the modal control force F_{mn}^c is rewritten as

$$F_{mn}^c = -\text{sign}(s)(\tilde{M}_{mnx} + \tilde{M}_{mny})\bar{S}(t) \tag{6}$$

where sign(·) is a signum function. In this paper, it is assumed that the remnant strain and electric field of actuators can disappear immediately when light direction is changed. With reference to Eq. (5), it can be seen that the switching function is determined by parameter c only. Therefore, how to determine the value of c is the next issue to be considered.

According to the VSC theory, c must be chosen in such a way that the existence and the reaching of the sliding mode are guaranteed. The mathematical form of this condition can be stated as

$$s\dot{s} < 0 \quad \text{or} \quad \begin{cases} \dot{s} < 0 & \text{if } s > 0 \\ \dot{s} > 0 & \text{if } s < 0 \end{cases} \tag{7}$$

Take the derivative of sliding surface with respect to time, then

$$\dot{s} = c\dot{\eta}_{mn} + \ddot{\eta}_{mn} \tag{8}$$

Substituting Eqs. (1) and (6) into Eq. (8), then

$$\begin{cases} \dot{s} = c\dot{\eta}_{mn} + \ddot{\eta}_{mn} = -(2\zeta_{mn}\omega_{mn} - c)\dot{\eta}_{mn} - \omega_{mn}^2\eta_{mn} + \left|F_{mn}^c\right| > 0 & \text{if } s < 0 \\ \dot{s} = c\dot{\eta}_{mn} + \ddot{\eta}_{mn} = -(2\zeta_{mn}\omega_{mn} - c)\dot{\eta}_{mn} - \omega_{mn}^2\eta_{mn} - \left|F_{mn}^c\right| < 0 & \text{if } s > 0 \end{cases} \tag{9}$$

Eq. (9) shows that only if the system state trajectory in phase plane moves into the region between the two lines L_1 and L_2 (see Fig. 2), the reaching conditions could be satisfied. This part of the area is known as the region of attraction. The lines L_1 and L_2 are formulated as

$$\begin{cases} L_1 : \omega_{mn}^2\eta_{mn} + (2\zeta_{mn}\omega_{mn} - c)\dot{\eta}_{mn} = \left|F_{mn}^c\right| \\ L_2 : \omega_{mn}^2\eta_{mn} + (2\zeta_{mn}\omega_{mn} - c)\dot{\eta}_{mn} = -\left|F_{mn}^c\right| \end{cases} \tag{10}$$

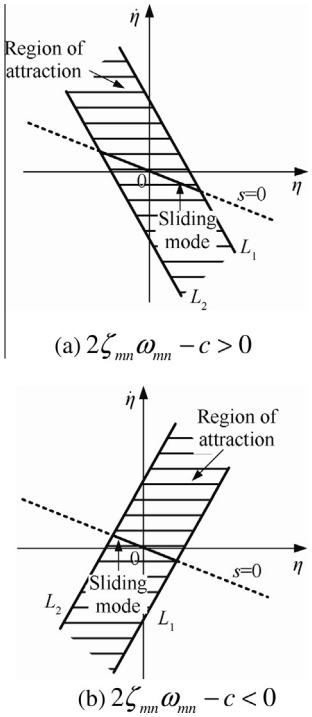

Fig. 2 Sliding mode.

As shown in Fig. 2, the switching line $s = 0$ located in the region of attraction is known as the sliding mode. With ideally switching control force F_{mn}^c, the system state trajectory could reach the sliding area in finite time. Once the system state trajectory slides towards the origin along the switching line, the vibration will be suppressed.[16] In the sliding mode area, system states satisfy $s = c\eta_{mn} + \dot{\eta}_{mn} = 0$, that is, $\dot{\eta}_{mn} = -c\eta_{mn}$. It is thus clear that $c > 0$ guarantees the stability of sliding mode motion. At the same time, the parameter c directly determines the sliding speed, and influences the range of the region of attraction; thereby affects the length of the sliding mode area. The length of the sliding mode area l is written as

$$l = \frac{2\left|F_{mn}^c\right|\sqrt{1+c^2}}{\left|\omega_{mn}^2 - 2\zeta_{mn}\omega_{mn}c + c^2\right|} \tag{11}$$

From Eq. (11), it can be seen that the length of the sliding mode area is proportional to the modal control force strength, thus increasing the intensity of the modal control force is always beneficial; For a flexible structure, $0 \leqslant \zeta_{mn} < 1$, the length of the sliding mode area is limited. When c equals to the product of ζ_{mn} and ω_{mn}, the maximum value of the length of the sliding mode area, which is most favorable to the vibration suppression, is obtained. Thus the expression of s can be rewritten as

$$s = \zeta_{mn}\omega_{mn}\eta_{mn} + \dot{\eta}_{mn} \tag{12}$$

3.2. Light intensity self-tuning fuzzy active control design

Designing light intensity self-tuning fuzzy active controller is shown in Fig. 3. The center of the plate ($x = L_x/2$ and $y = L_y/2$) is used as the reference point to evaluate control effectiveness. A laser Doppler vibrometer remotely measures the displacement of this reference point, which is used as the

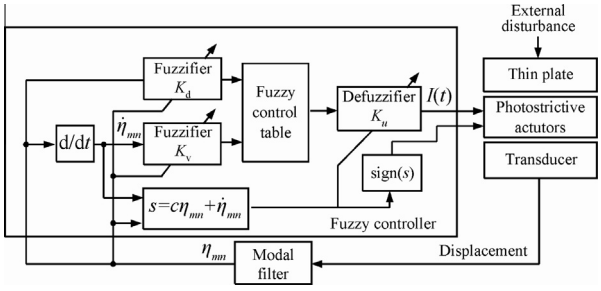

Fig. 3 System structure diagram.

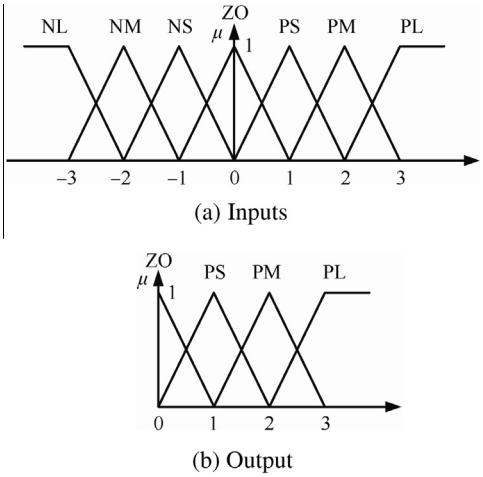

Fig. 4 Membership functions of the inputs and output.

feedback reference in a closed-loop control system. A modal filter (MF) is used to obtain the designated modal displacement for the vibration displacement sensed by the laser vibrometer. The designated modal displacement and its derivative are used to construct the sliding mode function and taken as fuzzy controller inputs. Here, the sign of the sliding mode function is taken as an index to decide which actuator should be irradiated. The designated modal displacement and velocity are multiplied by the scale factors K_d and K_v, respectively. The fuzzy output is determined from a look-up table. This fuzzy output is then assigned a numerical value which is multiplied by K_u to obtain the desired light intensity $I(t)$.

The system response only changes near the fuzzy linguistic value "ZO" when the displacement η_{mn} becomes very small in vibration. Meanwhile, the other fuzzy linguistic values clearly do not work in description and resolution for the displacement at the moment. Ideally, when the displacement decreases, fuzzy partition should also be able to fully describe and analyze small displacement changes, so as to improve the control system resolution capacity in a small range, which is required to real-time tuning for scaling factors. In the meantime, for the sake of most possibly increasing the modal control force, tuning law for fuzzifier factors, K_d and K_v, are selected as:

When $s = c\eta_{mn} + \dot{\eta}_{mn} = 0$

$$\begin{cases} K_\mathrm{d} = 3/\eta_{mn} \\ K_\mathrm{v} = 3/\eta_{mn}\omega_{mn} \end{cases} \tag{13}$$

Fuzzy scaling factors, K_d and K_v, are responsible for mapping inputs, the displacement η_mn and the velocity $\dot{\eta}_{mn}$, to the universe of discourse $[-3, 3]$.

Since vibration has been basically suppressed in the later stages of the vibration control, there is no need to impose control force, and then the light intensity should be reduced to zero. Therefore, tuning law for defuzzifier factors K_u is selected as

$$K_u = \frac{|s|}{|s| + \delta} \cdot \frac{I_\mathrm{max}}{3} \tag{14}$$

where $|s|$ is the absolute value of switching function $s = c\eta_{mn} + \dot{\eta}_{mn}$, I_max the provided maximum light intensity, and δ a small positive constant.

Fuzzy controller is designed as follows:

(1) *Selecting linguistic variables and membership functions.*

The chosen inputs of the fuzzy controller are the modal displacement η_{mn} and velocity $\dot{\eta}_{mn}$, which are defined on the universe of discourse $[-3, 3]$. The chosen output is the light intensity $I(t)$ irradiated on the photostrictive actuators. Considering that light intensity $I(t)$ is always positive, the output are defined on the universe of discourse $[0, 3]$. Accordingly, the set of linguistic values for the inputs are $\{\mathrm{NL}, \mathrm{NM}, \mathrm{NS}, \mathrm{ZO}, \mathrm{PS}, \mathrm{PM}, \mathrm{PL}\}$, and the output is $\{\mathrm{ZO}, \mathrm{PS}, \mathrm{PM}, \mathrm{PL}\}$. Here, NL, NM, NS, ZO, PS, PM and PL refer to negative large, negative medium, negative small, zero, positive small, positive medium and positive large, respectively. In this paper, the triangular membership functions shown in Fig. 4 are used, which fuzzify the set elements on the universe of discourse.

(2) *The establishment of the fuzzy control rules.*[15]

According to the fuzzy control rules, fuzzy output can be inferred from the inputs of the fuzzy. Usually, fuzzy control rules are based on the actual control experience. With reference to the history of vibration response, it is observed that, when $\eta_{mn} < 0$ and $\dot{\eta}_{mn} < 0$, control force F^c_{mn} imposed on the plate should be large. For the photostrictive actuators, in order to produce a large control force F^c_{mn}, control light intensity have to be large, corresponding to the fuzzy linguistic value PL; Similarly, when $\eta_{mn} > 0$ and $\dot{\eta}_{mn} > 0$, one of control light intensity should also be PL; Otherwise, when $\eta_{mn} < 0$ and $\dot{\eta}_{mn} > 0$, or $\eta_{mn} > 0$ and $\dot{\eta}_{mn} < 0$, there is no need to impose large control force on the plate, so one of control light intensity should be ZO, PS or PM; Through summing up the above-mentioned experience, the fuzzy control rules are shown in Table 1.

(3) *Defuzzification.*

The resulting fuzzy set must be converted to a single crisp value in order to form a control signal to the plant. In this paper, center of gravity (COG) method is adopted. The resulting defuzzified value is

$$u_\mathrm{COG} = \int_{\tilde{X}} \mu_{\tilde{x}}(\tilde{x})\tilde{x}\mathrm{d}\tilde{x} \Big/ \int_{\tilde{X}} \mu_{\tilde{x}}(\tilde{x})\mathrm{d}\tilde{x} \tag{15}$$

where $\tilde{x}$ is a point in the universe $\tilde{X}$ of the resulting fuzzy set, and $\mu_{\tilde{x}}(\tilde{x})$ the membership of the resulting conclusion set.

(4) *Building fuzzy control table.*

The basic idea of fuzzy control table is shown as follows. Firstly, fuzzy control table is built by means of inferring all possible control actions offline with discrete premise universes before putting the controller into operation. With two controller inputs and one output, the table is a two-dimensional lookup table. Secondly, fuzzy control table is stored in computer memory. Finally, when the fuzzy controller is put into operation, the computer only needs to look up the control table and pick the corresponding output scaling value in accordance with the scaling values of the sampling modal

Table 1 Fuzzy control rules.

η	$\dot{\eta}$						
	NL	NM	NS	ZO	PS	PM	PL
NL	PL	PL	PL	PM	ZO	ZO	ZO
NM	PL	PL	PL	PS	ZO	ZO	PS
NS	PL	PL	PL	ZO	ZO	PS	PM
ZO	PL	PM	PS	ZO	PS	PM	PL
PS	PM	PS	ZO	ZO	PL	PL	PL
PM	PS	ZO	ZO	PS	PL	PL	PL
PL	ZO	ZO	ZO	PM	PL	PL	PL

displacement η_{mn} and velocity $\dot{\eta}_{mn}$. The desired light intensity $I(t)$ is obtained by multiplying the lookup value by K_u. The pre-calculation improves execution speed, as the runtime inference is reduced to a table lookup.

In this paper, it is assumed that there is a resolution of 47 points in each universe, so the table holds 47^2 elements. In order to improve the control effect, the choice of 10 points is from the universe $[-3,-1]$ and $[1,3]$ with a step of 0.5, the choice of 18 points is from the universe $[-0.9,-0.1]$ and $[0.1,0.9]$ with a step of 0.1, and the choice of 19 points is from the universe $[-0.09,0.09]$ with a step of 0.01. That is to say, the smaller the control input value, the higher the resolution. Since the fuzzy control table holds too many elements, it is not given in detail. Fig. 5 illustrates a nonlinear control surface include 47^2 points, of which every four points constitute a rectangular plane. In addition, Fig. 5 suggests that the fuzzy control table is consistent with the fuzzy control rules.

3.3. Chattering reduction

The phenomenon of some oscillations in some vicinity of the switching surface is called chattering problem. Due to physical limitations in real-world systems, directly applying the control law shown in Eq. (6) usually leads to chattering problem. Chattering is undesirable, since it involves a high speed switching control activity to cause energy wasting, and furthermore may excite high-frequency dynamics neglected in the course of modeling. Chattering must be reduced for the controller to perform properly. This can be achieved by smoothing out the control discontinuity in a thin boundary layer.[16,17] In this paper, the following continuous function $\Delta(s)$ is used to approximate the sign function sign(s):

$$\Delta(s) = s/(|s| + \delta) \quad (\delta > 0) \tag{16}$$

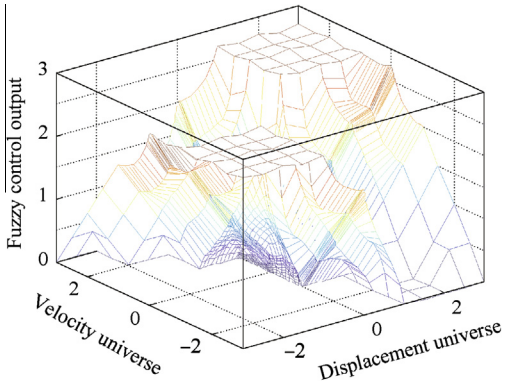

Fig. 5 Control surface.

4. Case study

In this section, one case study of active vibration control is performed for a simply supported plate to validate the effectiveness of the proposed control strategy. The dimensions of the controlled plate is $L_x = 0.8$ m, $L_y = 0.6$ m, and $h = 0.001$ m. The plate is assumed to be steel with material properties given as $Y = 2.1\times 10^{11}$ N/m^2, $\rho = 7.8\times 10^3$ kg/m^3 and $\mu = 0.3$. Two paired actuators, with the same dimension: 0.24 m $\times$ 0.06 m $\times$ 0.00025 m, are perfectly bonded on the top and bottom surfaces of the plate. The calibrated parameters of actuators from Ref.[6] are used for case study. In the arrangement, the corner coordinates or locations of the two paired actuators are $x_1^x = 0.05$ m, $x_2^x = 0.29$ m, $y_1^x = 0.24$ m, $y_2^x = 0.30$ m, $x_1^y = 0.34$ m, $x_2^y = 0.40$ m, $y_1^y = 0.06$ m, $y_2^y = 0.30$ m, respectively. Only the $(1,1)$ mode is taken as the sample mode to evaluate in closed-loop controls which are presented next. The exact natural frequency of $(1,1)$ mode is 10.705 Hz determined by the formula[6]

$$\omega_{mn} = \pi^2\sqrt{D/(\rho h)}\left[(m/L_x)^2 + (n/L_y)^2\right] \tag{17}$$

where D denotes the flexural rigidity of the plate.

For observing the time history of displacement response, an initial modal displacement of 1.0×10^{-3} m and an initial damping ratio 1% are imposed to the $(1,1)$ mode. With reference to Eq. (12), the switching function is

$$s = 0.6726\eta_{11} + \dot{\eta}_{11} \tag{18}$$

Applying the proposed chattering reduction scheme, the parameter δ takes a small positive constant 0.0001. However, since the modal control force varies with time, it is difficult to obtain an analytical solution of the modal equation. Thus, a classical numerical method, the Newmark-β method, is adopted to estimate discrete time responses.

With reference to Fig. 6, the settling times corresponding to the velocity feedback light intensity control and the proposed light intensity control are 3.5 and 2.2 s, respectively. It is obviously seen that the proposed light intensity control algorithm provides better control performance than the velocity feedback light intensity control. Fig. 7 shows that the modal control

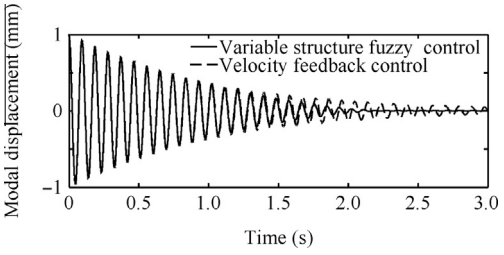

Fig. 6 Time history of displacement response.

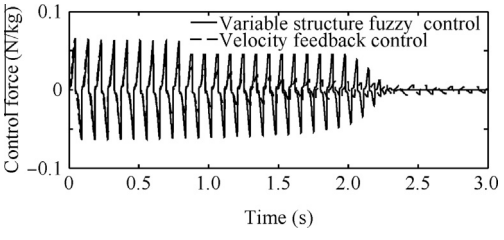

Fig. 7 Time history of control force.

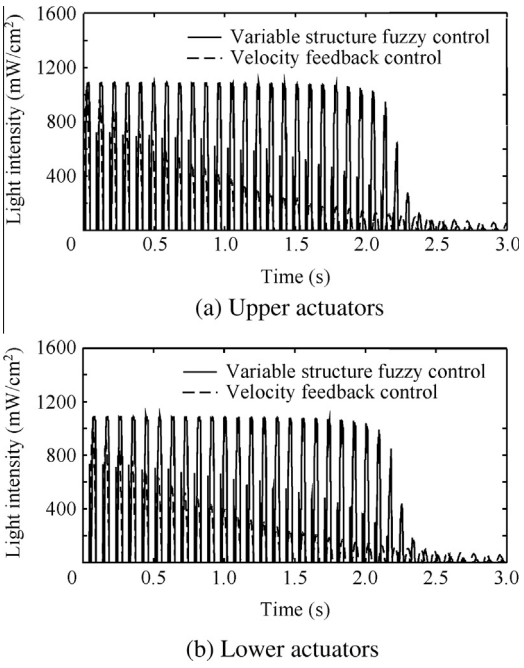

Fig. 8 Time history of control light intensity.

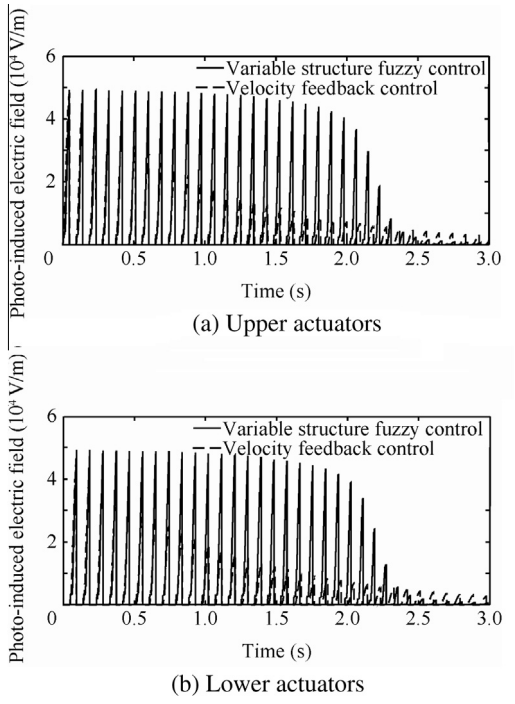

Fig. 9 Time history of photo-induced electric field.

force with the proposed control algorithm is greater than with the velocity feedback in the earlier stage of the vibration control (0–2 s), and is gradually reduced to zero with the light intensity being reduced to zero in the later stage. As seen in Fig. 8, due to the use of the proposed self-tuning law for fuzzifier factors K_d and K_v, greater light intensity is applied to the top and bottom actuators in the earlier stage of the vibration control (0–2 s). Meanwhile, it is also indicated that when the vibration is gradually suppressed, the system state trajectory

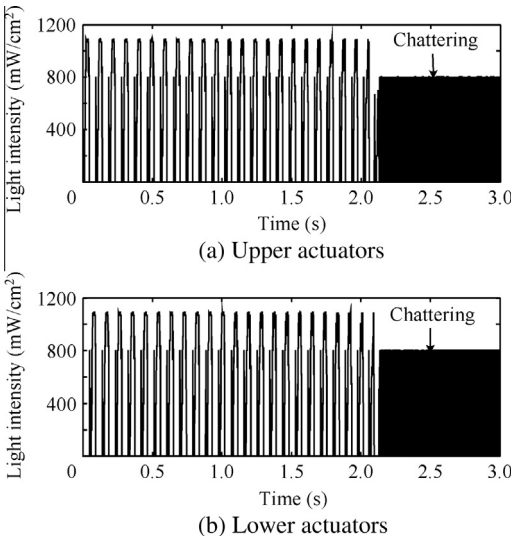

Fig. 10 Time history of control light intensity without chattering reduction.

approaches on the sliding surface. In this time $s \approx 0$, the light intensity is reduced to zero according to the tuning law for defuzzifier factors K_u. Fig. 9 shows that the amplitude of photo-induced electric field with the proposed control algorithm is much larger than that of the velocity feedback light control. The time history of control light intensity without chattering reduction is presented in Fig. 10. Comparing Fig. 10 with Fig. 8 suggests that chattering for the variable structure control is reduced by the introduction of the proposed chattering reduction method.

5. Conclusions

(1) In order to overcome nonlinear dynamic characteristics of photostrictive actuators, a variable structure self-adjusting parameter fuzzy control algorithm of light intensity is investigated, in which an idea of an off-line calculated fuzzy control table is adopted. The optimal switching surface is derived to increase the range of the sliding area to facilitate vibration suppression. Self-adjusting parameter scheme is applied.

(2) Compared with velocity feedback control, the proposed control strategy forces the actuators to produce greater modal control forces in the earlier stage of the vibration control, so suppresses the vibration more effectively. When vibration is effectively suppressed, the light intensity is reduced to zero.

(3) Due to the introduction of the proposed chattering reduction scheme, chattering for variable structure control is significantly reduced and thus the control quality of the system is improved.

Acknowledgement

This study was supported by National Natural Science Foundation of China (Nos. 10872090 and 50830201) and Qing Lan Project.

References

1. Tzou HS, Chou CS. Nonlinear opto-electromechanics and photodeformation of optical actuators. *Smart Mater Struct* 1996;**5**:230–5.
2. Shih HR, Tzou HS. Opto-piezothermoelastic constitutive modeling of a new 2-D photostrictive composite plate actuator. *Proc 2000 ASME Int Mech Eng Congr Exposition* 2000;**61**:1–8.
3. Liu B, Tzou HS. Distributed photostrictive actuation and opto-piezothermoelasticity applied to vibration control of plates. *ASME J Vib Acoust* 1998;**120**(4):937–43.
4. Shih HR, Smith R, Tzou HS. Photonic control of cylindrical shells with electro-optic photostrictive actuators. *AIAA J* 2004;**42**(2):341–7.
5. Shih HR, Watkins J, Tzou HS. Displacement control of a beam using photostrictive optical actuators. *J Intell Mater Syst Struct* 2005;**16**(4):355–63.
6. Shih HR, Tzou HS, Saypuri M. Structural vibration control using spatially configured opto-electromechanical actuator. *J Sound Vib* 2005;**284**(1–2):361–78.
7. Shih HR, Tzou HS. Photostrictive actuators for photonic control of shallow spherical shells. *Smart Mater Struct* 2007;**16**(5):1712–7.
8. Shih HR, Tzou HS, Walters W. Photonic control of flexible structures-application to a free-floating parabolic membrane shell. *Smart Mater Struct* 2009;**18**(11):1–7.
9. Wang XJ, Yue HH, Jiang J, Deng ZQ, Tzou HS. Wireless active vibration control of thin cylindrical shells laminated with photostrictive actuators. *J Intel Mater Syst Struct* 2011;**22**(4):337–51.
10. Yue HH, Sun GL, Deng ZQ, Tzou HS. Distributed shell control with a new multi-DOF photostrictive actuator design. *J Sound Vib* 2010;**329**(18):3647–59.
11. Sun D, Tong L. Theoretical investigation on wireless vibration control of thin beams using photostrictive actuators. *J Sound Vib* 2008;**312**(1–2):182–94.
12. Zheng SJ. Finite element simulation of wireless structural vibration control with photostrictive actuators. *Sci China Technol Sci* 2012;**55**(3):709–16.
13. Chen DJ, Zheng SJ. Genetic algorithm based LQR vibration wireless control of laminated plate using photostrictive actuators. *Earthquake Eng Eng Vib* 2012;**11**(1):83–90.
14. Takawa T, Fukuda T, Nakashima K. Fuzzy control of vibration of a smart CFRP laminated beam. *Smart Mater Struct* 2000;**9**(2):215–9.
15. Park KS, Koh HM, Seo CW. Independent modal space fuzzy control of earthquake-excited structures. *Eng Struct* 2004;**26**(2):279–89.
16. Sinha A, Kao CK. Independent modal sliding mode control of vibration in flexible structure. *J Sound Vib* 1999;**147**(2):352–8.
17. Utkin V. Variable structure system with sliding modes. *IEEE Trans Autom Control* 1977;**AC-22**(2):212–22.

He Rongbo received his M.S. degree from Harbin University of Science and Technology in 2005, and then became an instructor at Anhui University of Technology. He is currently a Ph.D. candidate at Nanjing University of Aeronautics and Astronautics (NUAA). His main research interest is wireless structure vibration control with photostrictive actuators.

Zheng Shijie received his Ph.D. degree in Engineering Mechanics from Dalian University of Technology in 1996, and then became a postdoctoral fellow at Nanjing University of Aeronautics and Astronautics. During postdoctoral research, he visited University of Hong Kong many times as a senior visiting scholar. Currently, he is a professor and a Ph.D. advisor in the College of Aerospace Engineering at Nanjing University of Aeronautics and Astronautics. His research interests include intelligent computing, health monitoring for composite materials and structures, mechanical analysis of photoelectric, piezoelectric and functionally gradient materials.